Localized Retinal Electrophysiological and Fundus Autofluorescence Imaging Abnormalities in Maternal Inherited Diabetes and Deafness

Caren Bellmann,[1,2] *Magella M. Neveu,*[1] *Hendrik P. N. Scholl,*[1,2] *Chris R. Hogg,*[1] *Pamela P. Rath,*[1] *Sharon Jenkins,*[2] *Alan C. Bird,*[1,2] *and Graham E. Holder*[1]

Purpose. To investigate retinal function in patients with maternally inherited diabetes and deafness (MIDD) and to correlate the findings with fundus autofluorescence (FAF) imaging.

Methods. FAF was imaged in five patients (age range, 49–60 years) confirmed to have the mitochondrial DNA nucleotide A3243G point mutation. Retinal function was measured by full-field (Ganzfeld) electroretinography (ERG) and pattern ERG, incorporating the International Society for Clinical Electrophysiology of Vision (ISCEV) standards. Multifocal ERG (mfERG) was also performed. For analysis of the mfERG data, five regional ring groups of equal eccentricity were formed. For each ring, the peak amplitude (defined as the difference between P1 and N1) and the implicit time of P1 were determined and compared with normative values.

Results. Visual acuity in the patients was between 20/20 and 20/40 (Early Treatment Diabetic Retinopathy Study [ETDRS] chart). Irregular increased FAF signals were observed adjacent to and between areas of atrophy of the retinal pigment epithelium (RPE). Ganzfeld ERGs were within normal limits in three patients. Pattern ERG was abnormal in five eyes of three patients. mfERG peak amplitude abnormalities were particularly present in rings 2 and 3 and were consistent with the distribution of FAF abnormalities. In all but one eye, no implicit times changes were present.

Conclusions. Significant mfERG abnormalities with normal Ganzfeld ERG are consistent with nonuniform damage to the central retina in MIDD, in keeping with the FAF findings. Reduced peak amplitudes with normal implicit times in the mfERG suggest localized loss of function and may indicate damage to the cone photoreceptor outer segments or cone photoreceptor loss in MIDD. (*Invest Ophthalmol Vis Sci.* 2004; 45:2355–2360) DOI:10.1167/iovs.03-1090

From [1]Moorfields Eye Hospital, London, United Kingdom; and the [2]Institute of Ophthalmology, London, United Kingdom.

Supported by the European Commission QLK6-CT2000-51262 (Marie Curie Individual Fellowship) and Faun-Foundation (CB); Deutsche Forschungsgemeinschaft Grant (DFG) Scho-73411-2, DFG Scho-734/2-1 (Heisenberg Grant), European Commission QLKRT-2001-02494 (Concerted Action Program PHOTAGE) (HPNS).

Submitted for publication October 2, 2003; revised February 7 and 27, 2004; accepted March 4, 2004.

Disclosure: **C. Bellmann**, None; **M.M. Neveu**, None; **H.P.N. Scholl**, None; **C.R. Hogg**, None; **P.P. Rath**, None; **S. Jenkins**, None; **A.C. Bird**, None; **G.E. Holder**, None

Presented at the annual meeting of the Association for Research in Vision and Ophthalmology, Fort Lauderdale, Florida, May 2003.

The publication costs of this article were defrayed in part by page charge payment. This article must therefore be marked "*advertisement*" in accordance with 18 U.S.C. §1734 solely to indicate this fact.

Corresponding author: Graham E. Holder, Department of Electrophysiology, Moorfields Eye Hospital, City Road, London EC1V 2PD, UK; graham.holder@moorfields.nhs.uk.

Maternal inherited diabetes and deafness (MIDD) may present with diabetes mellitus, neurosensory hearing loss, and retinal dystrophy. MIDD is caused by the most common mitochondrial DNA point mutation A3243G.[1] The disease is found in 1% to 2% of the diabetic population and was first reported in 1992.[1–3] Retinal fundus changes range from mildly abnormal pigmentation to extensive atrophy of the retinal pigment epithelium (RPE) at the posterior pole.[1,4–6] An early report of the present study suggested a specific fundus autofluorescence (FAF) pattern in MIDD, which showed an irregular increased FAF signal adjacent to and between areas of atrophy of the RPE (Rath PP, et al. *IOVS* 2002;43:ARVO E-Abstract 4345).

The pathogenesis of the retinal changes in MIDD is not yet clear. Morphologic studies in Kearns-Sayre syndrome and mitochondrial encephalomyopathy, lactic acidosis, and strokelike episodes (MELAS) syndrome, as examples of diseases caused by the mitochondrial A3243G mutation, revealed degeneration of photoreceptor outer segments and ultrastructural changes in the retinal pigment epithelium.[7–9] Previous electrophysiological findings in MIDD were unremarkable in most patients. However, they were restricted to full-field electroretinogram (ERG) and electrooculogram,[4,10–13] which would not be expected to show significant abnormality in dysfunction confined to the macula. Both clinical observation and FAF findings suggest a localized paracentral retinal involvement in MIDD so that topographic measurements are needed to determine fully the extent of retinal dysfunction. The multifocal ERG (mfERG) and the pattern ERG (PERG) are suitable measures of central retinal function.[14,15] In this study, we examined electrophysiological results, incorporating mfERG and PERG, and compared the findings with those of FAF imaging.

Methods

The diagnosis of MIDD was based on medical history and clinical appearance. All patients were confirmed to have the mitochondrial DNA nucleotide A3243G point mutation. Fundus changes were documented by fundus photography, and FAF imaging was performed. Visual acuity was measured using the ETDRS chart. Retinal function was determined by electrophysiological investigation.

The study was approved by the local ethics committee, and informed consent was obtained from each patient before entering the study. The tenets of the Declaration of Helsinki were followed.

FAF Imaging

FAF imaging was recorded with a confocal scanning laser ophthalmoscope (HRA; Heidelberg Engineering, Dossenheim, Germany). As described previously,[16,17] an argon blue laser with a wavelength of 488 nm was used for excitation. Emission was recorded at higher than 500 nm.

Before examination, the pupil of the study eye was dilated with phenylephrine 2.5% and tropicamide 1%. Recordings were performed with best image focus and after correction of refractive errors.

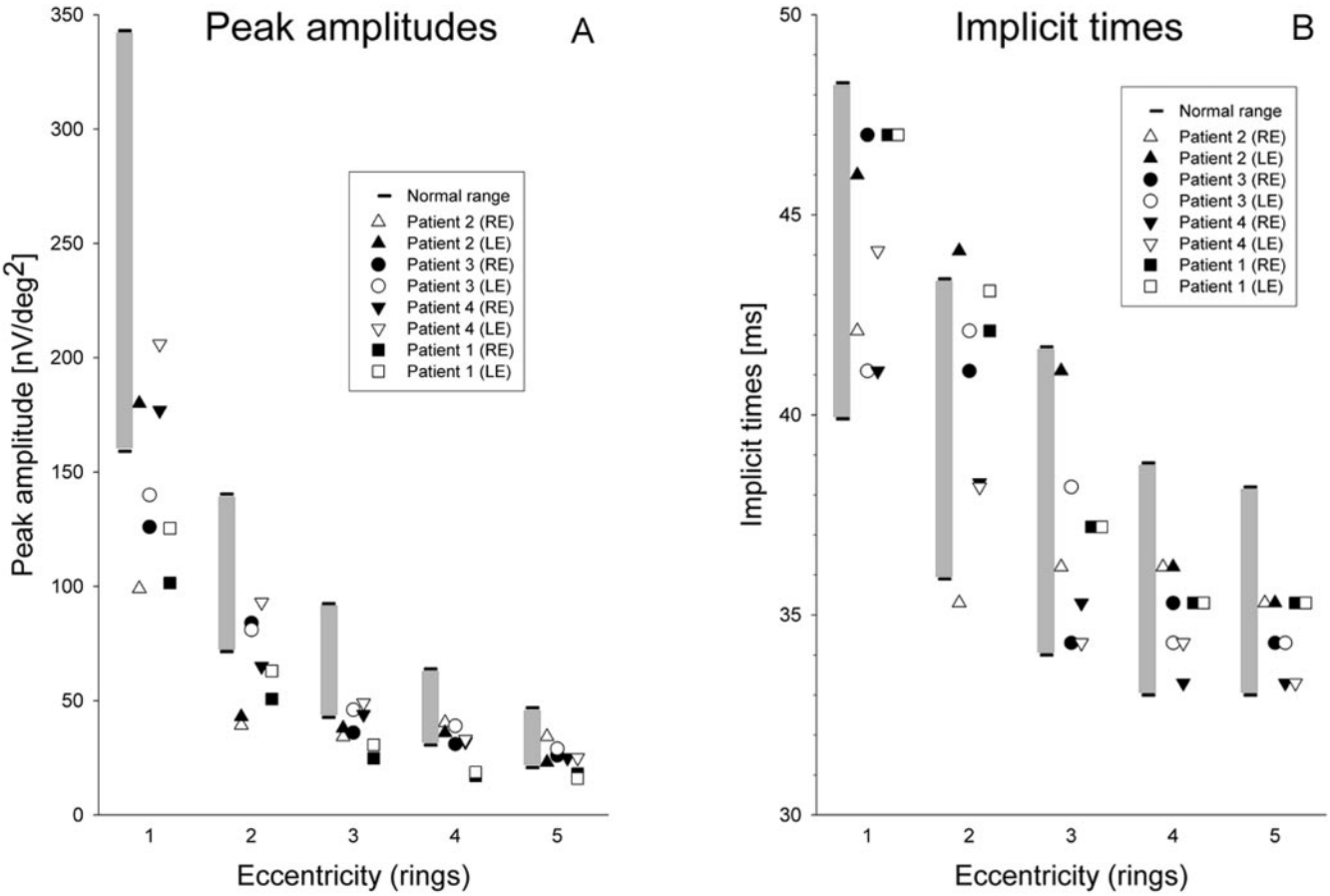

FIGURE 1. mfERG peak amplitudes (**A**) and implicit times (**B**) are shown for each eye of each patient. The normative values (5th–95th percentile) are shown as *gray boxes* between horizontal marks.

Electrophysiological Recordings

Assessment included Ganzfeld electroretinography (ERG) and PERG recorded incorporating the protocols recommended by the International Society for Clinical Electrophysiology of Vision (ISCEV).[18,19]

The mfERG was recorded with a commercial system (RETIscan System; Roland Consult, Wiesbaden, Germany). The stimulus used in the mfERG consisted of 61 hexagons, covering in total a visual field of 56.9°, at a viewing distance of 33 cm. The stimulus-distortion factor was set to 4 to compensate for differences in cone density across the retina, from center to periphery. Patients were asked to fixate on the center of a large cross in the central hexagon. Before examination, eyes were kept light adapted for at least 10 minutes. Pupils were dilated with phenylephrine 2.5% and tropicamide 1%. Average pupil diameter was 8 mm. Refractive errors were corrected. The mfERG was recorded binocularly in three patients and monocularly in one patient who had strabismus. One patient declined the mfERG.

All mfERG responses were recorded using corneal gold foil electrodes. The reference and ground electrodes were attached to the ipsilateral outer canthus and forehead, respectively. The surface electrode impedance was less than 5 kΩ. The signals were amplified and band-pass filtered (5–300 Hz; −3dB). Eight trials were recorded for each mfERG session, and the average recording time for each trial was 50 to 120 seconds. The total duration of a recording session was 20 minutes or less. These techniques are similar to those used in previous studies.[20,21]

The mfERG recordings were compared with FAF imaging results by superimposing the 61 trace arrays onto FAF images with external image analysis software (Photoshop 6.0; Adobe Systems, Mountain View, CA). In addition to qualitative analysis, further analyses were performed with the system (RETIscan; Roland) software. In particular, first-order kernels were considered for mfERG evaluation, because they correlate with the function of the outer retina.[15]

To reduce the complexity of the local 61 mfERG responses, five regional ring groups of equal eccentricity were formed. The ring groups were defined as follows: ring 1, from 0° to 2.1° eccentricity; ring 2, from 1.4° to 6.7° eccentricity; ring 3, from 5.7° to 12.0° eccentricity; ring 4, from 9.5° to 19.8° eccentricity; ring 5, from 15.1° to 28.5° eccentricity. For each ring group, the peak amplitude, defined as the difference between N1 and P1, was calculated, and the implicit time of P1 was determined. For analysis of the mfERG temporal data, the analysis was restricted to the implicit time of the positive deflection (P1). Results of peak amplitude and implicit time were compared with normative values ranging between the 5th and the 95th percentiles (Fig. 1).

RESULTS

Four female patients and one male patient were studied (age range, 49–60 years). All patients had significant neurosensory hearing loss. None showed signs of diabetic retinopathy, and all had stable glucose levels at the time of examination. The clinical data, together with Ganzfeld ERG and PERG are described in Table 1. mfERG results are demonstrated in Figure 1. In normal subjects, the amplitudes of each of the 61 local mfERG responses are almost equal, because of the stimulus scaling factor with increasing hexagon size toward the periphery, compensating for lower cone density (Fig. 2).

Patient 1

Visual acuity was 20/20 in both eyes. Fundus findings showed a symmetrical bilateral retinal involvement with irregular

TABLE 1. Visual Acuity and Electrophysiological Findings

No.	Age	Eye	VA	Ganzfeld ERG (30 Hz)		Rod-Specific b-wave		Pattern ERG Amplitude (P 50)
				Amplitude	Implicit time	Amplitude	Implicit Time	
1	52	RE	20/20	n	a	a	n	a
		LE	20/20	n	a	a	n	a
2	55	RE	20/40	n	n	n	n	a
		LE	20/32	n	n	n	n	a
3	49	RE	20/20	n	n	n	n	n
		LE	20/20	n	n	n	n	n
4	60	RE	20/25	n	n	n	n	n
		LE	20/25	n	n	n	n	n
5	56	RE	20/25	a	a	n	n	n
		LE	20/25	n	n	n	n	a

n, normal; a, abnormal.

patches of the retinal pigment epithelium atrophy at the posterior pole. The fovea was normal. FAF imaging revealed a decreased FAF signal in areas of RPE atrophy. An irregular increased FAF signal was observed adjacent to and between the areas of RPE atrophy.

Ganzfeld ERGs showed mildly subnormal rod-specific responses as well as subnormal maximal ERG a- and b-wave amplitudes from both eyes. The 30-Hz flicker ERG showed delayed implicit times but no amplitude abnormalities. The PERG amplitude was below the normal range indicating macular involvement. Although the mfERG showed reduced peak amplitudes with normal implicit times in all five ring groups (Fig. 1), mfERG changes were particularly present in areas of FAF abnormalities and without any substantial reduction in amplitude of the response to the central hexagon (Fig. 3A).

Patient 2

Visual acuity in the right eye was 20/40 and in the left eye 20/32. Extensive areas of RPE atrophy, sparing the fovea, were present in both eyes on ophthalmoscopy. The right eye was more severely affected, leaving only a small island centrally. A band of increased FAF adjacent to the RPE atrophy was observed in both eyes (Fig. 3B).

Scotopic and photopic Ganzfeld ERGs were bilaterally normal. The PERG was undetectable from the right eye, indicating severe maculopathy and reduced from the left eye.

mfERG evaluation revealed reduced peak amplitudes in ring groups 2 and 3 from both eyes and additionally in ring group 1 on the right corresponding to the areas of RPE atrophy (Fig. 1A). Implicit times were within the normal range in all ring

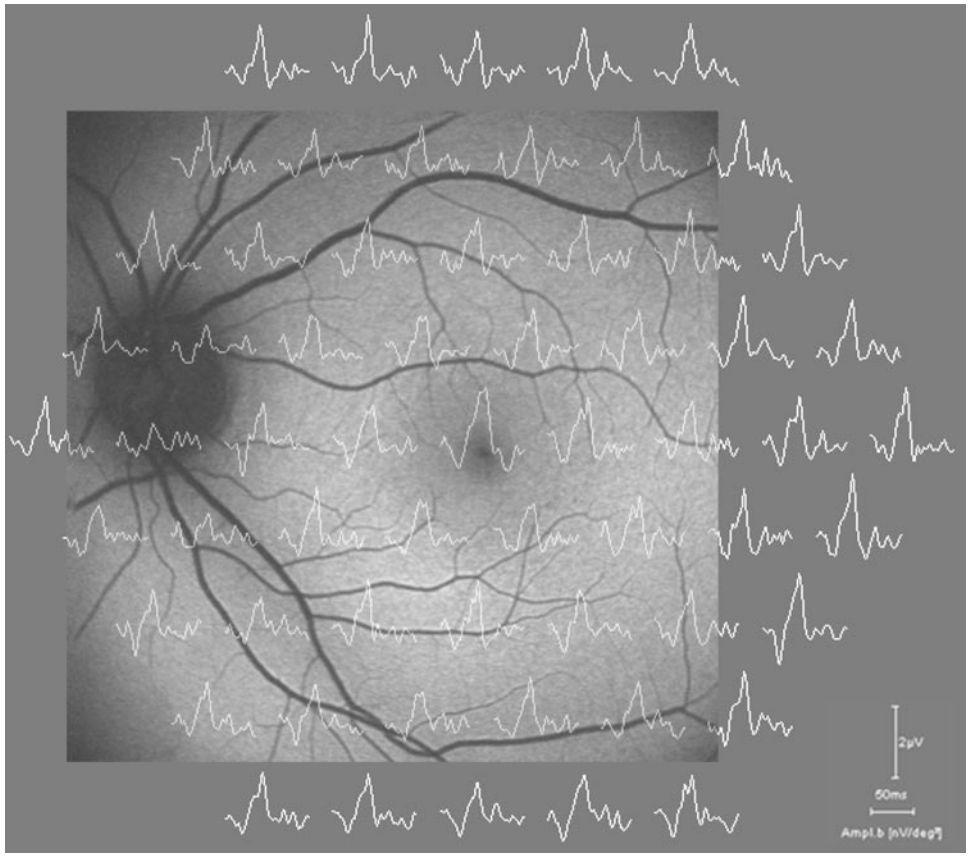

FIGURE 2. mfERG superimposed onto a FAF image in a normal subject (left eye). Amplitudes of the 61 local ERG responses are almost equal, because of the stimulus scaling with increasing hexagon size toward the periphery, compensating for lower cone density.

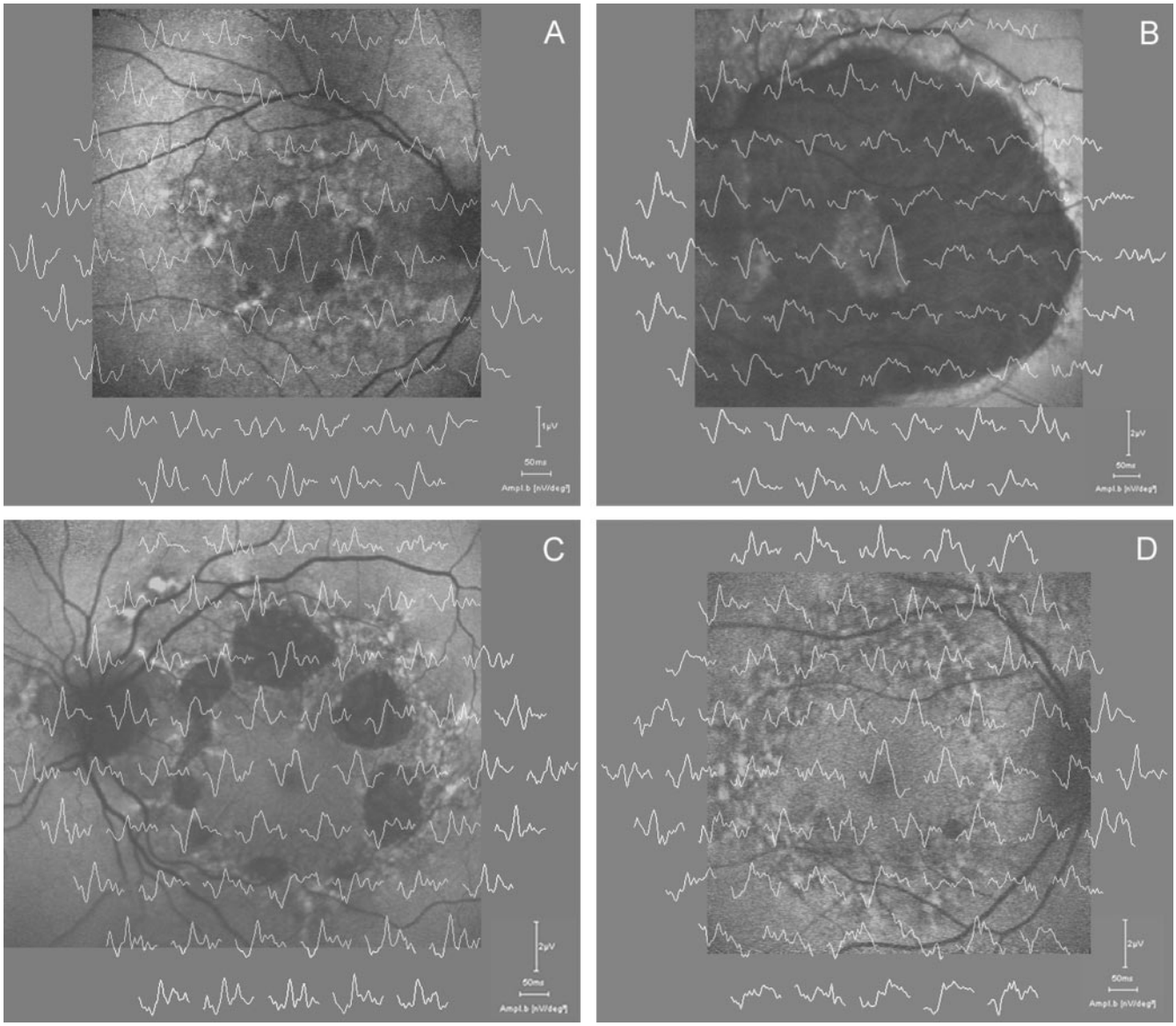

FIGURE 3. mfERG stimuli superimposed onto FAF images in patients with MIDD: (**A**) patient 1, (**B**) patient 2, (**C**) patient 3, and (**D**) patient 4. Trace arrays were changed in amplitude, particularly in areas of FAF signal change. No distinction could be made between areas of increased FAF and decreased FAF (RPE atrophy) using the 61-hexagon stimulus.

groups on the left eye and mildly delayed in the second ring group on the right (Fig. 1B).

Patient 3

Visual acuity was 20/20 in both eyes. Widespread areas of perimacular RPE atrophy were distributed in both eyes (Fig. 3C). The FAF signal was extinguished in areas of RPE atrophy, whereas an irregular increased FAF signal was found adjacent to and between the areas of atrophy. In comparison to patient 1 the fundus changes were located at greater eccentricity (Fig. 3A).

The Ganzfeld ERG was normal. Although the PERG was within the normal range in each eye, the mfERG showed reduced central peak amplitudes. In addition, peak amplitudes were reduced or borderline in ring group 3, whereas those in ring groups 2, 4, and 5 were normal. The implicit times were all normal (Fig. 1).

The overlay of the mfERG onto the FAF image is shown in Figure 3C. In comparison to areas with normal FAF background, the peak amplitudes were reduced both in areas of increased and decreased FAF. No distinction could be made between areas of RPE atrophy and areas with increased FAF.

Patient 4

The visual acuity measured in both eyes was 20/25. Areas of small RPE atrophy and pigmentary changes were seen on clinical examination bilaterally. The location and appearance of the fundus changes were similar to those described in patient 3, although the areas of RPE atrophy were more restricted. The FAF pattern was similar to that described before showing an irregular, increased FAF signal adjacent to and between the areas of RPE atrophy forming a ring-shaped pattern dystrophy at the posterior pole.

Ganzfeld ERG and PERG were normal. mfERG peak amplitudes were reduced only in ring group 2 from the right eye. The implicit times were normal in all rings (Fig. 1).

On visual inspection, the central hexagon showed no significant reduction, whereas reduced amplitudes were found in

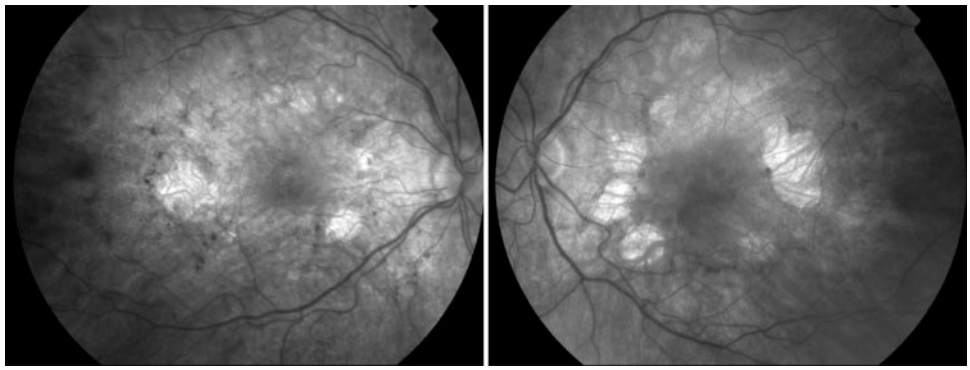

FIGURE 4. Fundus photographs of the left (*left*) and right (*right*) eyes of patient 5. Widespread perimacular RPE atrophy are distributed in both eyes. In the fovea drusenlike changes are present.

areas of increased and decreased FAF signals on both eyes (Fig. 3D).

Patient 5

The visual acuity in each eye was 20/25. Clinical examination revealed the typical changes of MIDD with perimacular RPE atrophy and pigmentary changes. Drusen-like changes were present in the fovea.

FAF images were similar to those in patient 3. A decreased FAF signal in areas of RPE atrophy and an increased FAF signal adjacent to and between these areas were observed.

The rod-specific Ganzfeld ERG was normal, whereas the 30-Hz cone flicker ERG showed delayed implicit times from both eyes and reduced peak amplitudes on the right eye. The PERG was normal in the right eye and but abnormal in the left (Fig. 4).

The patient declined mfERG examination.

DISCUSSION

Clinical examination and FAF imaging in MIDD revealed a typical pattern with areas of irregular increased FAF adjacent to and between the areas of RPE atrophy (Rath PP, et al. *IOVS* 2002;43:ARVO E-Abstract 4345) (Figs. 3, 4). The electrophysiological data revealed nonuniform central retinal dysfunction consistent with abnormalities suggested by FAF imaging. Only two patients demonstrated Ganzfeld ERG abnormalities suggestive of generalized retinal dysfunction, consistent with previous reports describing normal electrophysiology in most patients.[10–13,22] The Ganzfeld ERG, however, is a mass response and is thus unaffected by localized dysfunction such as a pure maculopathy.

The PERG and the mfERG are measures of central retinal function. A marked reduction in the amplitude of the PERG P50 component suggests dysfunction anterior to the ganglion cells in the visual pathway.[14] The PERG within the normal range in some of the patients is in keeping with localized retinal dysfunction surrounding the macular and sparing the fovea, as revealed both in fundus examination and FAF imaging. In other patients, there was sufficient retinal dysfunction to cause absolute abnormalities in the PERG.

The mfERG provides spatial information about the central retinal cones and their postreceptoral cells not readily available in the Ganzfeld ERG.[15] The mfERG has been used for investigation for a variety of macular diseases.[15,23–26] The present mfERG analysis in MIDD reveals reduction of peak amplitudes whereas the implicit times were normal in all but one eye. These findings are compatible with loss of cone photoreceptor outer segments as hypothesized by Hood.[15] One patient demonstrated a normal PERG, although the central hexagon of the mfERG showed reduced peak amplitudes. The mfERG may occasionally reveal subtle early changes in macular function that are not enough to produce an abnormal PERG.

In addition to the ring group analysis, we compared the mfERG results with FAF findings. With the 61-hexagon stimulus, mfERG responses were recorded over the optic nerve head. This is not an artifact. The hexagons do not fall completely on the optic disc, and light-scattering may contribute to the almost normal responses over the optic nerve head.[27] Qualitative analysis revealed no substantial peak amplitude reduction in the central element. Amplitude changes in the mfERG superimposed onto the FAF image corresponded well with the area of abnormality seen with FAF imaging (Fig. 3).

It is thought that an increased FAF signal is the result of a high metabolic turnover of photoreceptor outer segments leading to lipofuscin accumulation in RPE cells.[28] Both the electrophysiological and imaging data suggest restricted photoreceptor damage in MIDD rather than generalized retinal dysfunction. In histologic study of patients with A3243G mutation and Kearns-Sayre or MELAS syndrome, investigators reported atrophic photoreceptor outer segments and abnormal mitochondria in the inner retinal segments. Ultrastructural changes were present in RPE cells together with enlarged mitochondria.[7–9] It was postulated that photoreceptor outer segments are stressed both from the RPE and from photoreceptor inner segments, which contain 90% of the retina's mitochondria.[9,29]

Although the FAF pattern in MIDD is specific, the changes have similarities with the pattern described in patients with geographic atrophy due to age-related macular degeneration.[16] It is known that mitochondrial alterations are not only described in maternal inherited diseases but also appear in any aging postmitotic cell,[30] so that there may be a common pathogenic pathway in the development of atrophy of the RPE. Mitochondria are involved in a number of metabolic processes including the generation of chemical energy in form of adenosine triphosphate (ATP).[30] They are the main source of reactive oxygen species formation and important control centers for apoptosis.[30–32] Thus, it is no surprise that mitochondrial DNA shows a high mutation rate and that mutations accumulate with age.[33] Furthermore, defective mitochondria may be not properly autophagocytosed. Their components may undergo further oxidative modification within the lysosomes, resulting in the formation of additional undegradable material, such as lipofuscin in RPE cells, and progressively less mitochondrial recycling. Consequently, compensatory mechanisms may fail with time, followed by dysfunction and cell death, particularly in relation to postmitotic tissues with high energy demand, such as photoreceptors and RPE cells.[31]

Age-dependent somatic selection favors the persistence of mitochondria carrying the mutation in many mitochondrial diseases and symptoms may appear only later in life. This is in

keeping with the slow progression and localized damage in our patients and in patients with other mitochondrial diseases.[34]

Rod photoreceptor dysfunction may be predicted in patients with MIDD, as much of the generated energy in rods supports the ionic pumps that keep the cell in a response-ready state (i.e., for photoreceptor outer segment disc turnover and for the phototransduction cascade).[35] If rods were the first location susceptible to the effects of the A3243G mutation, it would explain the striking location of retinal changes, as histologic data describe a maximum rod density at 4 to 6 mm from the fovea.[36] Nevertheless, global rod system ERG abnormalities in the Ganzfeld ERG were observed in only one patient.

The results clearly demonstrate a nonuniform retinal damage and suggest damage to the cone photoreceptor outer segments in MIDD. The results support further the hypothesis that both photoreceptor outer segments and RPE cells are involved in the pathogenesis of MIDD, consistent with histologic data. However, whether the two cell layers are equally susceptible to the effects of the A3243G mutation or the photoreceptor damage is a consequence of the disease principally involving the RPE is yet to be ascertained.

Acknowledgments

The authors thank Alaric Smith for the referral of patients.

References

1. van den Ouweland JMW, Lemkes HHPJ, Ruitenbeek W, et al. Mutation in mitochondrial tRNA Leu (UUR) gene in a large pedigree with maternally transmitted type II diabetes mellitus and deafness. *Nat Gen*. 1992;1:368–377.
2. Ballinger SW, Shoffner JM, Hedaya EV, et al. Maternal transmitted diabetes and deafness associated with a 10.4kb mitochondrial DNA deletion. *Nature Genet*. 1992;1:11–15.
3. Guillausseau PJ, Massin P, Dubois-La Forgue D, et al. Maternal inherited diabetes and deafness: a multicenter study. *Ann Intern Med*. 2001;134:721–728.
4. Massin P, Guillausseau PJ, Vialettes B, et al. Macular pattern dystrophy associated with a mutation of mitochondrial DNA. *Am J Ophthalmol*. 1995;120:247–248.
5. Harrison TJ, Boles RG, Johnson DR, LeBlond C, Wong LJ. Macular pattern retinal dystrophy, adult-onset diabetes, and deafness: a family study of A3243G mitochondrial heteroplasmy. *Am J Ophthalmol*. 1997;124:217–221.
6. Souied EH, Sales MJ, Soubrane G, et al. Macular dystrophy, diabetes, and deafness associated with a large mitochondrial DNA deletion. *Am J Ophthalmol*. 1998;125:100–103.
7. McKechnie NM, King M, Lee WR. Retinal pathology in the Kearns-Sayre syndrome. *Br J Ophthalmol*. 1985;69:63–75.
8. Chang TS, Johns DR, Walker D, de la Cruz Z, Maumence IH, Green WR. Ocular clinicopathologic study of the mitochondrial encephalomyopathy overlap syndrome. *Arch Ophthalmol*. 1993;111:1254–1262.
9. Rummelt V, Folberg R, Ionescu V, Hwang T, Pe'er J. Ocular pathology of MELAS syndrome with mitochondrial DNA nucleotide 3243 point mutation. *Ophthalmology*. 1993;100:1757–1766.
10. Bonte CA, Matthijs GL, Cassiman JJ, Leys AM. Macular pattern dystrophy in patients with deafness and diabetes. *Retina*. 1997;17:216–221.
11. Latkany P, Ciulla TA, Cacchillo PF, Malkoff MD. Mitochondrial maculopathy: geographic atrophy of the macula in the MELAS associated A to G 3243 mitochondrial DNA point mutation. *Am J Ophthalmol*. 1999;128:112–114.
12. Smith PR, Bain SC, Good PA, et al. Pigmentary retinal dystrophy and the syndrome of maternally inherited diabetes and deafness caused by the mitochondrial DNA 3243 tRNA(Leu) A to G mutation. *Ophthalmology*. 1999;106:1101–1108.
13. Latvala T, Mustonen E, Uusitalo R, Majamaa K. Pigmentary retinopathy in patients with the MELAS mutation 3243A–>G in mitochondrial DNA. *Graefes Arch Clin Exp Ophthalmol*. 2002;240:795–801.
14. Holder GE. Pattern electroretinography (PERG) and an integrated approach to visual pathway diagnosis. *Prog Retin Eye Res*. 2001;20:531–561.
15. Hood DC. Assessing retinal function with the multifocal technique. *Prog Retin Eye Res*. 2000;19:607–646.
16. Holz FG, Bellmann C, Margaritidis M, Schütt F, Otto TP, Völcker HE. Patterns of increased in vivo fundus autofluorescence in the juncional zone of geographic atrophy of the retinal pigment epithelium associated with age-related macular degeneration. *Graefe's Arch Clin Exp Ophthalmol*. 1999;237:145–152.
17. Bellmann C, Rubin GS, Kabanarou SA, Bird AC, Fitzke FW. Fundus autofluorescence imaging compared with different confocal scanning laser ophthalmoscopes. *Br J Ophthalmol*. 2003;87:1381–1386.
18. Marmor MF, Zrenner E. Standard for clinical electroretinography (1999 update). *Doc Ophthalmol*. 1998–99;97:143–156.
19. Bach M, Hawlina M, Holder GE, et al. Standard for pattern electroretinography. International Society for Clinical Electrophysiology of Vision. *Doc Ophthalmol*. 2000;101:11–18.
20. Kutschbach E. Method for multifocal ERG using short length and corrected M-sequences. Wiesbaden: Roland Consult. Elektrophysiologische *Diagnostik Systeme*. 1997:1–11.
21. Palmowski A, Berninger T, Allgayer R, Andrielis H, Heinamnn-Vernaleken B, Rudolph G. Effects of refractive blur on the multifocal electroretinogram. *Doc Ophthalmol*. 1999;41–54.
22. Massin P, Virally-Monod M, Vialettes B, et al. Prevalence of macular pattern dystrophy in maternally inherited diabetes and deafness. GEDIAM Group. *Ophthalmology*. 1999;106:1821–1827.
23. Kretschmann U, Seeliger M, Ruether K, Usui T, Zrenner E. Spatial cone activity distribution in diseases of the posterior pole determined by multifocal electroretinography. *Vision Res*. 1998;38:3817–3828.
24. Kretschmann U, Seeliger M, Ruether K, Usui T, Apfelstedt SE, Zrenner E. Multifocal electroretinography in patients with Stargardt's macular dystrophy. *Br J Ophthalmol*. 1998;82:267–275.
25. Scholl HP, Schuster AM, Vonthein R, Zrenner E. Mapping of retinal function in Best macular dystrophy using multifocal electroretinography. *Vision Res*. 2002;42:1053–1061.
26. Nagasaka K, Horiguchi M, Shimada Y, Yuzawa M. Multifocal Electroretinograms in cases of central areolar choroidal dystrophy. *Invest Ophthalmol Vis Sci*. 2003;44:1673–1679.
27. Marmor MF, Hood DC, Keating D, Kondo M, Seeliger MW, Miyake Y (for the International Society for Clinical Electrophysiology of Vision). Guidelines for basic multifocal electroretinography (mfERG). *Doc Ophthalmol*. 2003;106:105–115.
28. Rückmann Av, Fitzke FW, Bird AC. Distribution of fundus autofluorescence with a scanning laser ophthalmoscope. *Br J Ophthalmol*. 1995;79:407–412.
29. Wolbarsht M, George G, Shearin WA Jr, Kylstra J, Landers M III. Retinopathy of permaturity: a new look into old disease. *Ophthalmic Surg.* 1983;14:919–924.
30. Wallace DC. Mitochondrial diseases in man and mouse. *Science.* 1999;5:283:1482–1488.
31. Wallace DC. Diseases of the mitochondrial DNA. *Annu Rev Biochem*. 1992;61:1175–1212.
32. Kroemer G, Reed JC. Mechanisms of mitochondrial membrane permeabilization. *Cell Death Differ*. 2000;7:1145.
33. Rustin P, von Kleist-Retzow JC, Vajo Z, Rotig A, Munnich A. For debate: defective mitochondria, free radicals, cell death, aging-reality or myth-ochondria? *Mech Ageing Dev*. 2000;114:201–206.
34. Yoneda M, Chomyn A, Martinuzzi A, Hurko O, Attardi G. Marked replicative advantage of human mtDNA carrying a point mutation that causes the MELAS encephalomyopathy. *Proc Natl Acad Sci USA.* 1992;89:11164–11168.
35. Futterman S. Metabolism and photochemistry in the retina. In: Moses R, ed. *Adlers Physiology of the Eye*. St. Louis: CV Mosby; 1975:406–419.
36. Curcio CA, Sloan KR, Kalina RE, Hendrickson AE. Human photoreceptor topography. *J Comp Neurol*. 1990;292:497–523.